# EMISSION SPECTRA OF THE NOBLE-GAS HALIDES: THE B(1/2)–A(1/2) SYSTEM

M.P. CASASSA, M.F. GOLDE and A. KVARAN‡
*Department of Chemistry, University of Pittsburgh, Pittsburgh, Pennsylvania 15260, USA*

Received 28 July 1978

The B(1/2)–A(1/2) transition has been detected in the emission spectra of ArBr, KrBr, KrI and XeI at low pressure. Comparison with the well-known "B–X" continua implies that, in many cases, the latter is heavily overlapped by C(3/2)–A(3/2) emission.

## 1. Introduction

The diatomic noble-gas halides were recently discovered through their chemiluminescence arising from the reactions of electronically-excited Ar, Kr and Xe ($^3P_{0,2}$) atoms with a variety of halogen-containing molecules [1,2]. These reactions are of great interest in that the excited atoms show certain properties similiar to those of ground state alkali atoms and the noble-gas halides have acquired importance as the basis of a group of high-power near-UV and vacuum-UV lasers.

The properties of the noble-gas halides have been studied theoretically and also through their absorption and emission spectra. Ab initio calculations [3–5] show that three close-lying excited states, B($\Omega = 1/2$), C(3/2) and D(1/2) can emit by $\Delta\Omega = 0$ transitions to the lower states, X(1/2), A(3/2) and A(1/2) (see schematic potential curves, fig. 1). Of these, the B–X, C–A(3/2) and D–X systems have been observed [6,7].

Interpretation of the experimental spectra has been most successful for XeF and XeCl where vibrational and, for XeF, rotational analysis of the B–X and D–X spectra have given information about the bound upper and lower electronic states [8,9]. In the other molecules, where the lower states are largely unbound, the emission spectra are continuous and assumptions concerning the assignments of the various features in the spectra have been necessary in order to allow analysis of the spectra [10].

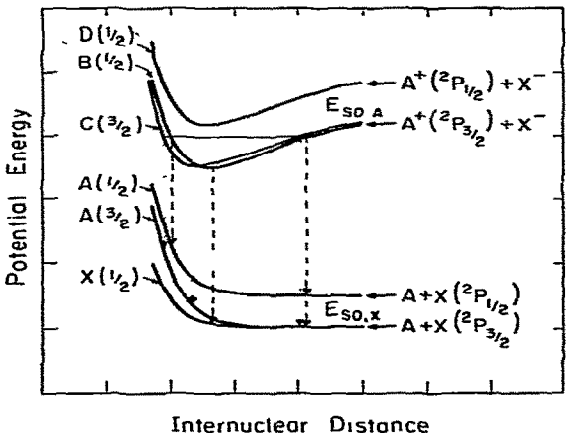


Fig. 1. Schematic potential curves for the noble-gas halides, AX. $E_{SO,A}$ (cm$^{-1}$): Ar: 1432; Kr: 5371; Xe: 10537. $E_{SO,X}$ (cm$^{-1}$): Br: 3685; I: 7603. ——— Transitions from B(1/2), . . . transitions from C(3/2).

In the present work, we report observation of B(1/2)–A(1/2) emission spectra in ArBr, KrBr, KrI and XeI. By comparing this new emission with the B–X and C–A(3/2) continua, we obtain evidence for appreciable overlap of B–X and C–A(3/2) emission in the "main continuum" of the spectrum.

## 2. Experimental

Spectra were generated in a discharge-flow apparatus by the reaction of metastable Ar, Kr and Xe

‡ Also Department of Chemistry, University of Edinburgh, Edinburgh, UK.

atoms ($A^{*3}P_{0,2}$) with bromine- and iodine-containing molecules (RX):

$$A^* + RX \rightarrow AX^* + R, \quad (1)$$

$$AX^* \rightarrow A + X + h\nu. \quad (2)$$

The metastable excited atoms were produced by flowing prepurified Ar, pure or with small admixtures of Kr or Xe, through a weak dc discharge at a total pressure of 0.5 to 12 torr. This flow was mixed with a small flow of reagent molecules, emerging from a concentric tube and the emission from the mixing zone was monitored with a vacuum monochromator (Hilger E766 one-meter normal incidence or Minuteman 305 MV 1/2-meter Czerny–Turner) and photomultipliers (EMR 542G for wavelengths less than 185 nm and EMI 9789QB for the range 150 to 500 nm).

The spectral responses of the detection systems were measured using band and continuous spectra of known spectral distribution. For the vacuum-UV, the ArCl B–X continuum ($Ar^* + Cl_2$, $CCl_4$), and the $H_2(B\,^1\Sigma_u^+ - X\,^1\Sigma_g^+)$, $N_2(a\,^1\Pi_g - X\,^1\Sigma_g^+)$ and $CO(A\,^1\Pi - X\,^1\Sigma^+)$ band systems were used and, for the near UV, $NO(A\,^2\Sigma^+ - X\,^2\Pi)$, $N_2(C\,^3\Pi_u - B\,^3\Pi_g)$ and $CO(a\,^3\Pi - X\,^1\Sigma^+)$. The spectra presented here have been corrected, where necessary, for spectral response.

Gaseous reagents, HBr and HI (Matheson), were trapped at 77 K and pumped on to remove volatile impurities, then were passed through a cooled, 195 K, trap at low pressure to remove condensable impurities. $CHBr_3$, $CBr_4$, $CH_3I$ and $CH_2I_2$ (Aldrich Chemical Co.) and $Br_2$ and $I_2$ (Mallinckrodt Inc.) were used without purification.

## 3. Results

The reactions of Ar, Kr and Xe metastable ($^3P_{0,2}$) atoms with $Br_2$, $I_2$, HBr, HI, $CH_2Br_2$, $CHBr_3$, $CBr_4$, $CH_3I$ and $CH_2I_2$ were studied. The dominant component of the gas was always Ar, the other components normally comprising at most a few percent of the flow. Low pressure spectra are presented in figs. 2 to 5; these include the first published spectra of KrI and ArBr.

The emission spectra arising from the reactions of Ar* with all the iodides and of Kr* with $I_2$ and $CH_2I_2$ consisted only of atomic lines from energetically-accessible excited states of iodine, populated by dissociative excitation of the reagent molecule. Kr* + HI, however, gave three distinct regions of continuous emission, as shown in fig. 2, which are referred to, from low to high wavelength, as the main continuum (MC), secondary continuum (SC) and third continuum (TC) and were assigned as principally B(1/2)–X(1/2), C(3/2)–A(3/2) and B(1/2)–A(1/2) respectively. The very intense $I(6s\,^4P_{5/2} - {}^2P_{3/2})$ line at 183 nm provided the low wavelength limit of this spectrum; other much weaker I lines

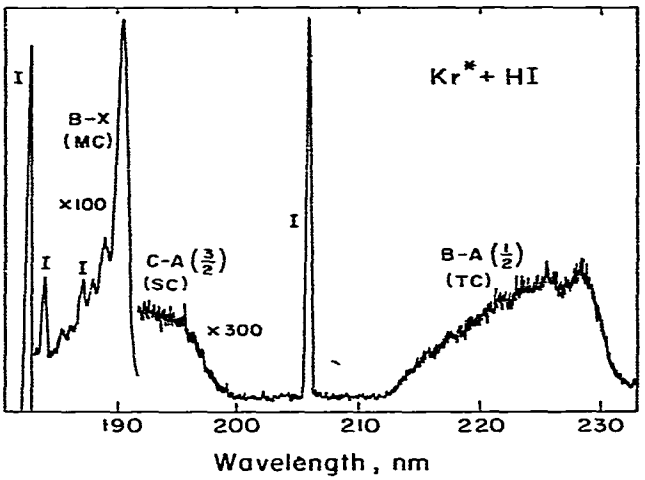


Fig. 2. KrI* spectrum generated by Kr* + HI at 2.1 torr total pressure. Iodine lines at 184.5, 187.6 and 206.2 nm arise from Ar* + HI.

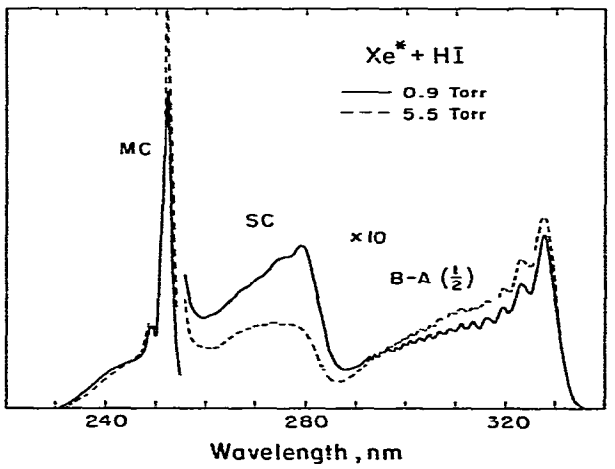


Fig. 3. XeI* spectra generated by Xe* + HI. Integrated intensities at the two pressures are equal.

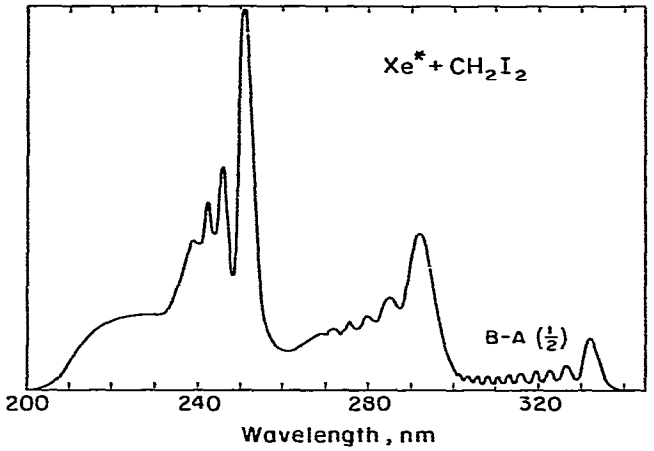


Fig. 4. XeI* spectrum generated by Xe* + $CH_2I_2$. Total pressure: 0.8 torr.

arise from the reaction of HI with residual traces of Ar*.

Spectra of Xe* with $CH_3I$, $CH_2I_2$ and HI showed no I* emission; again, the three XeI continua could be clearly distinguished (figs. 3 and 4).

For the reactions of Kr* with HBr and the bromomethanes, the MC and SC of KrBr were clearly resolved, but the B–A(1/2) system appeared as a shoulder at the long wavelength end of the C–A(3/2) continuum; structure, in the form of a separate peak at 228 nm, was apparent only in the case of Kr* + HBr.

The spectra of ArBr in fig. 5 are composites of

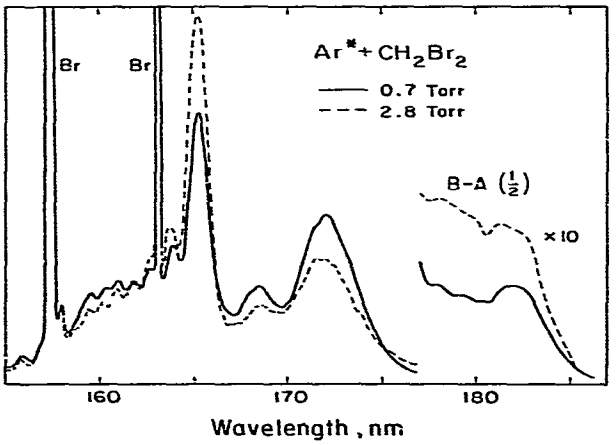


Fig. 5. ArBr* spectra generated by Ar* + $CH_2Br_2$. The integrated intensities at the two pressures are equal.

data obtained with both detection systems used in this study: the B–A(1/2) continuum is only partially resolved from the strong SC in the Ar* + $CH_2Br_2$ and HBr spectra. In the spectrum from Ar* + HBr, a further weak continuum was observed, extending from the tail of the B–A(1/2) system at 185 nm to at least 330 nm. The considerable structure in the ArBr continua will be discussed in a separate publication.

The dependence of the form of the spectra on total Ar pressure was investigated in order to confirm the B–A(1/2) assignments. For Xe* + HI, the ratio of the integrated XeI MC intensity to that of the B–A(1/2) continuum varied little with increasing pressure (fig. 6), while the SC intensity dropped markedly relative to that of the MC, due to electronic quenching of the C state.

Fig. 5 shows spectra of the Ar* + $CH_2Br_2$ reaction at 0.7 and 2.8 torr, the spectra being normalized to yield equal total integrated intensities. Both the B–A(1/2) region and MC peak show a positive pressure dependence, while the whole SC drops in intensity as the pressure is raised. Further data in table 1

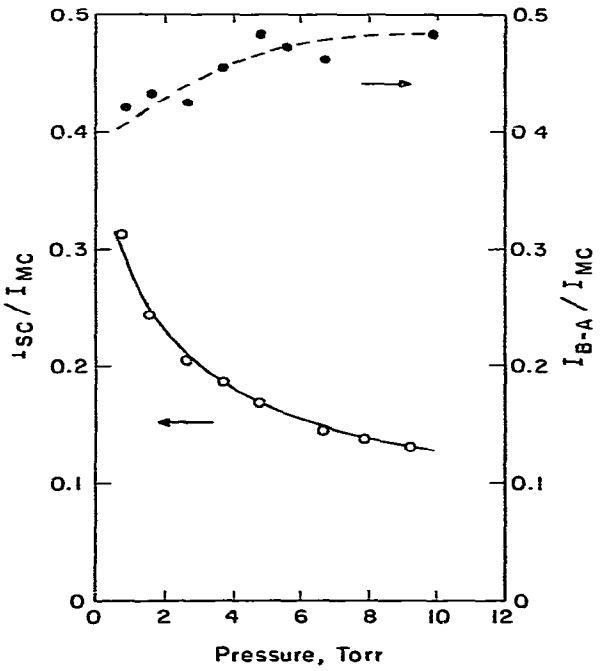


Fig. 6. Pressure dependence of the main continuum, secondary continuum and third continuum (B–A(1/2)) in XeI* (Xe* + HI). • $I_{B-A}/I_{MC}$; ○ $I_{SC}/I_{MC}$.

Table 1
Pressure dependence of the C–A(3/2) and B–A(1/2) continua relative to the main continuum in ArBr* from the reaction of Ar* with $CH_2Br_2$

| $p$ (torr) | $\frac{I(172.0\text{ nm})}{I(165.2\text{ nm})}$ | $\frac{I(179.0\text{ nm})}{I(165.2\text{ nm})}$ | $\frac{I(182.0\text{ nm})}{I(165.2\text{ nm})}$ |
|---|---|---|---|
| 0.45 | 0.78 | 0.027 | 0.030 |
| 0.77 | 0.59 | 0.029 | 0.031(5) |
| 1.33 | 0.45 | 0.033 | 0.033 |
| 1.78 | 0.37 | 0.034(5) | 0.033 |
| 2.34 | 0.31 | 0.038 | 0.034 |
| 3.06 | 0.25 | 0.040 | 0.035 |
| 3.75 | – | 0.042 | 0.035 |

confirm that the pressure dependence at 182 nm in the third continuum is closely similar to that of the B–X peak at 165.2 nm. No strong pressure dependence of the form of the KrI spectrum was observed over the range 1 to 4 torr, but the other systems studied showed behavior comparable to that of Xe* + HI and ArBr.

## 4. Discussion

### *4.1. Assignment of the B–A(1/2) system*

Ab initio calculations [3–5] have provided much of the present knowledge concerning the electronic states of the noble-gas halides. The potential curves of the excited B(1/2) and C(3/2) states are predicted to be similar in shape and position but there is as yet no definite experimental information as to their relative positions. Calculations and experiments [7] find that the D(1/2) state is displaced to higher energy by approximately the spin–orbit splitting of the noble-gas positive ion.

Calculations and experiment further agree that the A(3/2) state is considerably more repulsive than the X(1/2) ground state [5,10,11]. The A(1/2) state lies above the A(3/2) state by the halogen atom spin–orbit splitting at large internuclear distance; an atoms-in-molecule model calculation for KrF [3] found the A(1/2) and A(3/2) components to converge slowly at smaller internuclear distances to a limiting energy separation of two-thirds of that in the free atom.

The schematic potential curves, fig. 1, constructed on the basis of the above, imply that the B–A(1/2) bound–free continuum is expected to resemble that of the C–A(3/2) system in shape but to be shifted to long wavelength by approximately the halogen spin–orbit splitting. As shown in fig. 1, the limiting low and high wavelength regions of these continua should involve transitions close to the outer and inner turning-points respectively from the highest populated vibrational levels of the emitting states.

Applying these principles to the experimental spectra, in KrI (fig. 2), the highest emitting levels are determined by predissociation of the B and C states by states correlating with $Kr(^1S_0) + I^*(^4P_{5/2})$ (not shown in fig. 1). The threshold of the C–A(3/2) system is thus defined approximately by the wavelength, 183.0 nm, of the $I(^4P_{5/2}–^2P_{3/2})$ line. The low wavelength threshold of the B–A(1/2) continuum is 213.3 ± 0.2 nm, a displacement of 7750 ± 40 $cm^{-1}$ from the iodine line. This value is close to the spin–orbit splitting of the I atom, 7603 $cm^{-1}$.

Similarly, in the Xe* + HI spectrum, the predicted B–A(1/2) threshold is at 280.8 ± 0.6 nm, close to the lowest wavelength, 285 nm, at which B–A(1/2) emission can be resolved from the overlapping C–A(3/2) system.

In all the other noble-gas halides, the B–A(1/2) low wavelength threshold lies in the region of strong C–A(3/2) or B–X emission.

The long wavelength limits of the KrI B–A(1/2) and C–A(3/2) continua are similarly separated by an energy close to the iodine spin–orbit splitting. For XeI, KrBr and ArBr, however, this separation, although not accessible to precise measurement, is always somewhat smaller than the halogen spin–orbit splitting. We ascribe this to small differences in the B- and C-state potentials and in the A(3/2) and A(1/2) potentials, as discussed above (see fig. 1).

In conclusion, the wavelength ranges of the third continua are consistent with either B- or C-state emission to the A(1/2) state and the pressure dependences of the spectra (figs. 5 and 6 and table 1) establish the emitting state as the B(1/2) state.

The structure in the "third continua" is also consistent with this assignment. The broad oscillations in the ArBr and Xe* + $CH_2I_2$ spectra and at the long wavelength end of the Xe* + HI spectrum are quantum oscillations analogous to those in the C–A(3/2) spectrum [10], arising from the overlap of upper and lower state wavefunctions near the inner turning

points of the potential curves. The structure in the low wavelength region of the Xe* + HI B–A(1/2) spectrum is due to emission near the outer turning-point; each emitting vibrational level gives rise effectively to a separate peak and the spacing, approximately 110 $cm^{-1}$, between peaks is close to the vibration frequency of the analogous alkali halide, CsI.

The branching ratio for B-state emission to the X and A(1/2) states can be estimated from the Kr*, Xe* + HI spectra, showing that the B–A(1/2) system accounts for approximately 20% of the B-state emission in KrI and XeI.

For the bromides, the B–A(1/2) continuum is best resolved in ArBr; the resolved portion in the Ar* + HBr spectrum accounts for over 10% of the total B-state emission.

The iodides and bromides thus show very different behavior to KrF, for which calculations predict the B–A(1/2) system to be weaker than the B–X by a factor of about 30 [3].

*4.2. Composition of the main continuum*

Analysis of the noble-gas halide spectra is of interest for two reasons: to obtain potential curves for these novel species and to determine the vibrational distributions in the emitting states. This is especially important for spectra at low pressure ($\ll$1 torr), where the unrelaxed distributions give information concerning the dynamics of the formation reactions (1). The present results have an impact on both these aspects, in providing the first instance, in the noble-gas halides, of two band systems arising from a single excited electronic state.

Previous analyses of the MC of KrF at low pressure [10] and of several other noble-gas halides at high pressure [12] have assumed that the entire emission within this region can be assigned to the B–X system. A surprising result of the present study of ArBr and XeI was that the ratio of the B–A(1/2) intensity to that of the MC shows a small but definite positive pressure dependence. For Xe* + HI (fig. 6), where integrated intensities in the MC and B–A(1/2) continua were measured, the change in the ratio is about 20% between 1 and 5 torr.

For ArBr (Ar* + $CH_2Br_2$), the enhancement with pressure of the resolved B–A(1/2) emission relative to the peak of the MC, which itself shows a strong positive pressure dependence, is very striking (fig. 5 and table 1); the ratio of the B–A(1/2) intensity at 179 nm to the MC peak rises by more than 50% between 0.45 and 3.75 torr.

These results are consistent with a significant contribution of C state emission to the MC region. This is not unexpected as the C–A(3/2) low-wavelength threshold coincides with that of the B–X system (see fig. 1) and the spectra for Xe* + $CH_2I_2$ and Ar* + $CH_2Br_2$ (figs. 4 and 5) show strong C–A(3/2) emission right up to the long wavelength edge of the strong peak of the MC.

That the C–A(3/2) emission extends strongly to low wavelength under the MC can be deduced from the two Xe* + HI spectra in fig. 3, referring to 0.8 and 5.6 torr. The decrease in C–A(3/2) emission intensity as the pressure is increased is due to electronic quenching of the C(3/2) to the B(1/2) state. This is seen to result in an intensity enhancement of almost the whole B–A(1/2) spectrum, consistent with enhanced population of all but the highest emitting levels of the B state (which may be depleted by vibrational relaxation). In contrast, only the long wavelength peak of the MC shows a comparable enhancement, showing that at lower wavelength, particularly in the range 240–250 nm, quenching of contributing C-state emission is offsetting most of the enhancement of B–X emission.

In terms of the potential curves of fig. 1, this portion of C–A(3/2) emission arises from transitions near the outer turning-point of the C-state potential curve. Strong emission may result, despite the fact that the electronic transition moment for C–A(3/2) has been calculated to decrease sharply with increasing internuclear distance [3,5], because of the strong $\nu^5$ dependence of intensity on transition frequency, $\nu$, when the spectra are plotted, as here, on a wavelength scale. For high vibrational levels, the outer turning-point in the C state occurs at very large internuclear distances; in these cases (e.g. Xe* + $CH_2I_2$), the low wavelength region probably also includes C–X emission, whose transition moment may exceed that of C–A(3/2) in this region [3].

We have calculated C–A(3/2), X spectra for KrF, for which calculated molecular properties are available; these show that emission from high vibrational levels in fact reaches a separate intensity maximum at

low wavelength, in the region of the MC. This behavior is supported by the observed spectra of several noble-gas halides, in which strong C—A(3/2) emission in the SC is accompanied by a pronounced hump or shoulder in the low-wavelength region of the MC. Examples include $Xe^* + CH_2I_2$ (fig. 4), $Kr^* + CBr_4$ and $CHBr_3$, and $Ar^* + CCl_4$.

The possible presence of appreciable C-state emission particularly at low pressures must be considered when analyzing the MC in terms of the dominant B—X system. For the low-pressure ArBr spectrum produced by $Ar^* + CH_2Br_2$, for instance, the MC cannot be simulated in terms of B—X transitions alone. However, in other cases such fits to the MC may be possible but will give erroneous results for the B and X state potential curves and the B state vibrational distribution unless the C—A(3/2) contribution is allowed for.

Additionally, in deriving vibrational distributions in the B state, both the B—X and B—A(1/2) continua must be analyzed; because of the strong and very different dependence of transition moments on internuclear distance for these two transitions [3], the partitioning of emission between the B—X and B—A(1/2) systems may change markedly with vibrational quantum number.

## Acknowledgement

We acknowledge the Donors of the Petroleum Research Fund, administered by the American Chemical Society, the Research Corporation and the Royal Society for support of this research. We are also indebted to Dr. R.J. Donovan for the loan of a monochromator for experiments performed at the University of Edinburgh.

## References

[1] M.F. Golde and B.A. Thrush, Chem. Phys. Letters 29 (1974) 486.
[2] J.E. Velazco and D.W. Setser, J. Chem. Phys. 62 (1975) 1990.
[3] P.J. Hay and T.H. Dunning, J. Chem. Phys. 66 (1977) 1306.
[4] M. Krauss, J. Chem. Phys. 67 (1977) 1712.
[5] E.W. McDaniel, M.R. Flannery, H.W. Ellis, F.L. Eisele, W. Pope and T.G. Roberts, Compilation of Data Relevant to Rare Gas–Rare Gas and Rare Gas–Monohalide Excimer Lasers, Technical Rept H-78-1, U.S. Army Missile Research and Development Command (1977) Vol. 1.
[6] J. Tellinghuisen, G.C. Tisone, J.M. Hoffman and A.K. Hays, J. Chem. Phys. 64 (1976) 4796.
[7] J.E. Velazco, J.H. Kolts and D.W. Setser, J. Chem. Phys. 65 (1976) 3468.
[8] J. Tellinghuisen, J.M. Hoffman, G.C. Tisone and A.K. Hays, J. Chem. Phys. 64 (1976) 2484.
[9] P.C. Tellinghuisen, J. Tellinghuisen, J.A. Coxon, J.E. Velazco and D.W. Setser, J. Chem. Phys. 68 (1978) 5187.
[10] K. Tamagake and D.W. Setser, J. Chem. Phys. 67 (1977) 4370.
[11] M.F. Golde, J. Mol. Spectry. 58 (1975) 261.
[12] J. Tellinghuisen, A.K. Hays, J.M. Hoffman and G.C. Tisone, J. Chem. Phys. 65 (1976) 4473.